

Pore Deformation of Shale under Supercritical Carbon Dioxide based on MIP

Baobao Wang¹

¹Oil and Natural Gas Engineering, Chongqing University of Science and Technology, Chongqing 401331, China

wbbstudy [at] 163.com

Abstract: *This paper studies the characteristics of pore changes before and after supercritical CO₂ action, and discusses the influence of supercritical CO₂ action on shale pores. Taking the shale of the Silurian Longmaxi Formation in the eastern Sichuan Basin as the experimental sample, the MIP experiment was used to analyze the process of mercury in and out of shale before and after the action of supercritical CO₂, and changes in pore structure of shale after supercritical CO₂ treatment. The mercury injection amount of shale after supercritical CO₂ treatment increases significantly. Because of the extraction reaction and dissolution reaction with shale pore surface minerals after supercritical CO₂ injection, some micropores and mesopores are transformed into mesopores and macropores through dissolution, and new micropores are generated, resulting in the increase of mesopore PV and macropore SSA in shale. Ultimately, experiments have shown that supercritical CO₂ can expand the average pore size of shale and improve the seepage channels inside the shale, thereby enhancing shale oil recovery.*

Keywords: Shale, Supercritical CO₂, Pore Deformation, MIP

1. Introduction

Nowadays, with the surge in global energy demand, the consumption of crude oil is increasing day by day, and the application of CO₂ in unconventional resource extraction has attracted more and more attention of various countries. China is rich in shale oil resources and can be regarded as an important replacement resource for conventional oil and gas resources to make up for the lack of supply and demand of conventional oil and gas resources in China^[1]. However, due to the complex geological characteristics of shale oil reservoirs and the influence of supercritical CO₂ on shale pores^[2-3], the efficiency of carbon dioxide extraction of shale oil is not high in recent years, and it is not worth economic development. Shale oil reservoirs have low porosity, low permeability, strong sensitivity, and poor reservoir fluid availability^[4-5]. Its microscopic characteristics mainly include pore geometry and pore size, which are important parts of exploring pore deformation in shale reservoirs^[6-10]. For oil shale reservoirs with micro-nano pore size, reservoir mineral composition, pore structure and pore size distribution, reservoir physical properties and other factors play a decisive role in the storage capacity of crude oil in shale reservoirs. Therefore, in recent years, scholars from various countries have taken CO₂-action shale reservoir regular pore structure characteristics as a breakthrough point, and opened up new research directions for improving shale oil recovery^[11].

The main research methods for quantitative characterization of pores include MIP and low-temperature adsorption (CO₂, N₂). In this study, MIP experiments are mainly used as characterization methods^[12-13]. The technology will be

introduced below. High-pressure mercury injection is a method of using mercury porosimeter to press mercury into porous media under different pressure conditions to obtain pore structure characteristics. It is also the most commonly used method for measuring capillary pressure at home and abroad. High-pressure mercury injection is to increase the mercury injection pressure on the basis of conventional mercury intrusion technology^[14-16], and can detect the pore volume with a radius between 1.8nm and 500um. Based on MIP experiments, this paper studies the characteristics of pore changes before and after supercritical CO₂ action, and investigates the effect of supercritical CO₂ action on shale pores.

2. Experimental Section and Methods

2.1 Sample preparation

The samples for this experimental study were collected from the reservoir shale of the Silurian Longmaxi Formation in the East Sichuan Basin, with a burial depth of 4325-4357m. The device used in the sample preparation process is a self-developed shale soaking device, as shown in Fig.1. The main components of the device are a dryer, a high-precision ISCO pump, a reaction tank and a sensor. The sample preparation process is as follows: (1) According to the full-diameter shale core, a 25mm standard core column was drilled, and the core was cleaned with an ultrasonic core oil washing machine. (2) Put the rock sample into an oven set to 110°C for drying, take out the core, place it in a cooler, cool

it to room temperature, and measure the dry weight, length and diameter of the core. (3) The shale core is crushed into particles with a particle size of 3mm and placed in the reaction tank, and a certain amount of CO₂ is introduced into the reaction tank. In order to ensure that CO₂ was in supercritical state, MIP experiment was carried out by reaction at 8MPa and 50°C for 15 days.

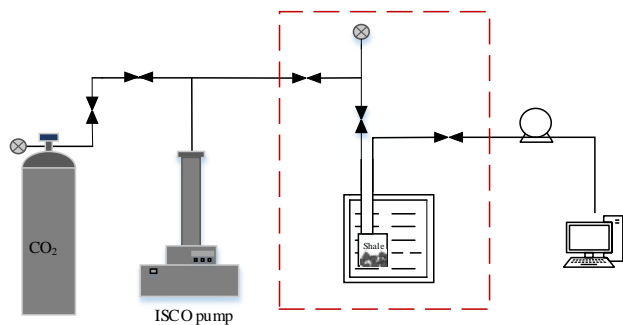


Figure 1: Supercritical CO₂- shale immersion device

2.2 MIP Analysis

The MIP test uses a PoreMaster-33 automatic mercury porosimeter (Canta Instruments, USA), which mainly realizes the determination of the specific surface area SSA, pore volume (PV) and pore size distribution (PSD) by measuring the advance and retreat mercury curves of shale, and the pore size is determined. The range is 6.4nm~950um, and the pressure range is from vacuum to 420MPa.

3.Results and Discussion

3.1Mercury intrusion and extrusion curve

MIP is widely used in quantitative characterization of shale structure. The two curves in Fig.2 describe the process of mercury injection and ejection in shale before and after supercritical CO₂ extraction. 1-2 is the initial low pressure. When $P < 0.2$ MPa, the amount of mercury injection increases rapidly with the increase of pressure, which mainly characterizes the pore volume between particles. 2-3 is the intermediate slowly rising stage. When $0.2 \text{ MPa} < P < 45$ MPa, the mercury injection curve increases gently with the pressure, and the mercury injection amount mainly reflects the pore volume in the particle. After stage3 is the end of the rising section, when $45 \text{ MPa} < P < 420 \text{ MPa}$, with the increasing pressure, the volume of shale particles is compressed, and the micropores in the shale matrix are also broken through by high mercury pressure, resulting in rapid growth of mercury injection.

MIP curve can reflect the development and connectivity of pores in shale. The original volume of mercury injection in shale is 0.0025ml/g, after supercritical CO₂ extraction, the volume of mercury injection in shale is 0.0063 mL / g.

Compared with the original shale, the mercury injection volume increased by 1.5 times, indicating that the pore volume of shale after supercritical CO₂ extraction increased greatly. The mercury ejection curve has obvious lag, indicating that some mercury remains in the shale. On the one hand, there are pores of ink bottle shape in the sample, resulting in a general decrease in mercury extrusion efficiency. On the other hand, there is a certain interfacial tension between mercury and shale pore throat surface, resulting in partial retention of mercury.

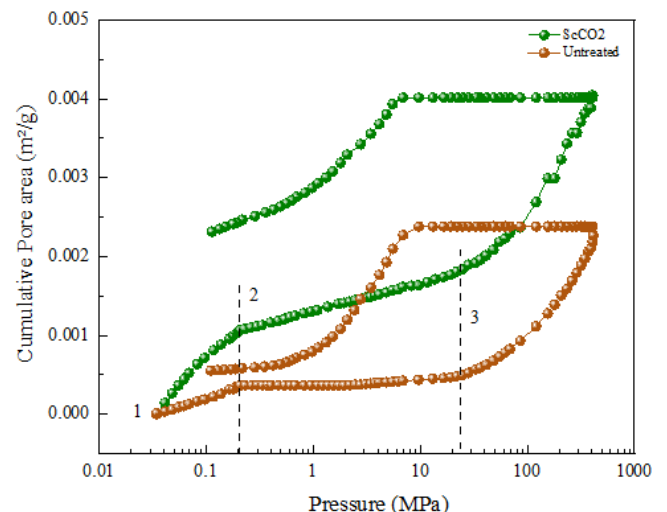


Figure 2: Mercury intrusion and extrusion curves before and after ScCO₂ treatment

3.2 Changes of the pore-structure parameters based on MIP

The SSA and PV of various pores in shale before and after treatment are shown in Table.1. The MIP data show that the original shale samples mainly contain mesopores and macropores, in which the volume of mesopores and macropores accounts for 56% and 44% of total pores. After supercritical CO₂ extraction, the volume of mesopores increased significantly, accounting for 60.32% of total pores. For SSA, in the original shale sample, the mesopore occupies the majority of SSA, accounting for about 99.15% of TSSA, while the macropore SSA only accounts for 0.85%. After supercritical CO₂ extraction, the macropore SSA increased significantly, about 1.14%, while the mesopores SSA decreased to 98.86%. The average pore size Ra increased from 8.63nm to 11.27nm, which may be due to the extraction and dissolution reaction between supercritical CO₂ injection and the mineral on the pore surface of shale. Some micropores and mesopores were transformed into mesopores and macropores through dissolution, and new micropores were generated, resulting in the reduction of macropore PV and the increase of mesopore SSA, and the increase of average pore size, which expanded the seepage channel inside the shale.

Table 1: SSA, PV and pore diameter of all kinds of pores based on MIP

Treatment methods	SSA (m ² /g)	Macro-	TSSA	PV (cm ³ /g)	Macro-	TPV	Ra (nm)
	Meso-			Meso-			
Untreated	0.7798	0.0067	0.7865	0.0014	0.0011	0.0025	8.63
ScCO ₂	1.9761	0.0228	1.9989	0.0038	0.0025	0.0063	11.27

4. Conclusion

In this paper, shale samples from Longmaxi Formation of Silurian in Eastern Sichuan Basin are taken as experimental samples. MIP experiments are used to analyze the process of mercury injection and ejection before and after supercritical CO₂ technique, and the changes of shale pore structure after supercritical CO₂ extraction. The main conclusions are as follows:

- (1) Mercury intrusion and extrusion curve results show that the mercury injection of shale after supercritical CO₂ technique increases significantly, indicating that the pore volume of shale after supercritical CO₂ extraction. The obvious lag of mercury ejection curve indicates that there are ink bottle pores in the sample, resulting in a general decrease in mercury ejection efficiency, and the interfacial tension between mercury and shale pore throat surface can also lead to partial retention of mercury.
- (2) Due to the extraction and dissolution reaction between supercritical CO₂ injection and shale pore surface minerals, some micropores and mesopores are transformed into mesopores and macropore through dissolution, and new micropores are generated. Therefore, the PV of the mesopores and SSA of the macropore increase.
- (3) Supercritical CO₂ technique can expand the average pore size of shale and improve the seepage channel inside shale, thereby improving the recovery ratio of shale oil.

Acknowledgement

This study was funded by the Chongqing Graduate Scientific Research Innovation Project (NO.CYS21495), the Postgraduate Innovation Program of Chongqing University of Science and Technology (NO.YKJXCX2020116), the Postgraduate Innovation Program of Chongqing University of Science and Technology (NO.YKJXCX2020124), the Postgraduate Innovation Program of Chongqing University of Science and Technology (NO. YKJXCX2120116), and the Postgraduate Innovation Program of Chongqing University of Science and Technology (NO.YKJXCX2020117).

Reference

- [1] Choquette P W, Pray L C. 1970. Geologic nomenclature and Classification of porosity in sedimentary carbonates [J].AAPG Bulletin, 54 (2): 278-298.
- [2] Bennett R H, O'Brien N R, Hulbert M H.1991. Determinants of clay and shale microfabric signatures: Processes and mechanisms.Microstructure of Fine-Grained Sediments:From mud to shale [C]. New York: Springer-Verlag, 5-32.
- [3] Jarvie D M, Hill R J, Ruble T E, et al. 2007. Unconventional shale-gas systems: The Mississippian Barnett Shale of north-central Texas as one model for thermogenic shale-gas assessment [J]. AAPG Bulletin, 91 (4): 475-499.
- [4] Singh P, Slatt R, Borges G, et al. 2009. Reservoir characterization of unconventional gas shale reservoirs: Example from the Barnett Shale, Texas, USA [J]. Oklahoma City Geological Society, 60 (1): 15-31.
- [5] Simon R, Graue D. Generalized correlations for predicting solubility, swelling and viscosity behavior of CO₂-crude oil systems [J]. Journal of Petroleum Technology. 1965, 17: 102-106.
- [6] Passey Q R, Bohacs K M, Esch W L, et al.2010.From oil-prone source rock to gas-producing shale reservoir-Geologic and petrophysical characterization of unconventional shale gas reservoirs [C]. The CPS/SPE International Oil &Gas Conference, Beijing, China, June 8~10, SPE Paper 131350, 29p.
- [7] Bustin R M, Bustin A M, Cui X, et al.2008. Impacts of shale properties on pore structure and storage characteristics [C]. Shale Gas Production Conference, Fort Worth, TX, November 16~18, SPE Paper 119892.
- [8] Bernard S, Horsfield B, Schulz HM, et al. 2012. Geochemical evolution of organic-rich shales with increasing maturity: A STXM and TEM study of the Posidonia shale (Lower Toarcian, northern Germany) [J]. Marine and Petroleum Geology, 31 (1): 70-89.
- [9] Slatt R M, O'Brien N R, Molinares-Blanco C, et al. 2013. Pores, Spores, Pollen and Pellets: Small, but Significant Constituents of Resource Shale [C].Unconventional Resources Technology Conference, Denver, United States, August 12th, 630-642.
- [10] Saidian M, Kuila U, Rivera S, et al. 2014. Porosity and pore size distribution in mudrocks: a comparative study for Haynesville, Niobrara, Monterey and Eastern European Silurian Formations [C]. The unconventional Resources Technology Conference, Denver, Colorado, August 25~27, URTEC: 1922745, 18p.
- [11] Smith J R, Chen A, Gostovic D, et al. 2009. Evaluation of the relationship between cathode microstructure and electrochemical behavior of SOFCs [J]. Solid State Ionics, 180 (1): 90-98.
- [12] Sondergeld C H, Ambrose R J, Rai C S, et al. 2010.Microstructural studies of gas shales [C].Society of Petroleum Engineers Unconventional Gas Conference, Pittsburgh, Pennsylvania, February 23~25, 2010, SPE Paper 131771, 17p.
- [13] Javadpour F.2009. Nanopores and apparent permeability of gas flow in mudrocks (shales and siltstone) [J]. Journal of Canadian Petroleum Technology, 48 (8):16-21.
- [14] Langmuir I.1917. The constitution and fundamental

- properties of solids and liquids, Part 1, Solids [J].
Journal of the Franklin Institute, 184 (5): 102-105.
- [15] Brunauer S, Emmett P H, Teller E. 1938. Adsorption of gases in multimolecular layers [J]. Journal of the American Chemical Society, 60 (2): 309-319.
- [16] Krohn C E. 1988. Sandstone fractal and euclidean pore volume distributions [J]. Journal of Geophysical Research Atmospheres, 93 (B4): 3286-3296.